

# ACP++: Action Co-occurrence Priors for Human-Object Interaction Detection

Dong-Jin Kim, *Member, IEEE*, Xiao Sun, *Member, IEEE*,  
Jinsoo Choi, *Member, IEEE*, Stephen Lin, *Member, IEEE*, In So Kweon, *Member, IEEE*,

**Abstract**—A common problem in the task of human-object interaction (HOI) detection is that numerous HOI classes have only a small number of labeled examples, resulting in training sets with a long-tailed distribution. The lack of positive labels can lead to low classification accuracy for these classes. Towards addressing this issue, we observe that there exist natural correlations and anti-correlations among human-object interactions. In this paper, we model the correlations as *action co-occurrence matrices* and present techniques to learn these priors and leverage them for more effective training, especially on rare classes. The efficacy of our approach is demonstrated experimentally, where the performance of our approach consistently improves over the state-of-the-art methods on both of the two leading HOI detection benchmark datasets, HICO-Det and V-COCO.

**Index Terms**—Human-object interaction, visual relationship, co-occurrence, label hierarchy, knowledge distillation.

## I. INTRODUCTION

HUMAN-object interaction (HOI) detection aims to localize humans and objects in an image and infer the relationships between them. An HOI is typically represented as a human-action-object triplet with the corresponding bounding boxes and classes. Detecting these interactions is a fundamental challenge in visual recognition that requires both an understanding of object information and high-level knowledge of interactions.

A major issue that exists in HOI detection is that its datasets suffer from long-tailed distributions, in which many HOI triplets have few labeled instances. Similar to datasets for general visual relationship detection (VRD) [53], a reason for this is missing labels, where the annotation covers only a subset of the interactions present in an image. For the widely-used HICO-Det dataset [3], 462 out of the 600 HOI classes have fewer than 10 training samples. For such classes, the lack of positive labels can lead to inadequate training and low classification performance. In particular, since the supervision for the layer weights is mostly 0 for rare classes, confusion occurs for these classes. How to alleviate performance degradation on rare classes is thus a key issue in HOI detection.

To address the problem of long-tailed distributions, we propose to take advantage of natural *co-occurrences* in human actions. In other words, given a pair of a human and an object,

D. Kim, J. Choi, and I. S. Kweon are with the School of Electrical and Computer Engineering, KAIST, Daejeon, Republic of Korea.

E-mail: {dijnjusa,jinsc37,iskweon77}@kaist.ac.kr

X. Sun and S. Lin are with the Visual Computing group, Microsoft Research, Beijing, China.

E-mail: {xias,stevelfin}@microsoft.com

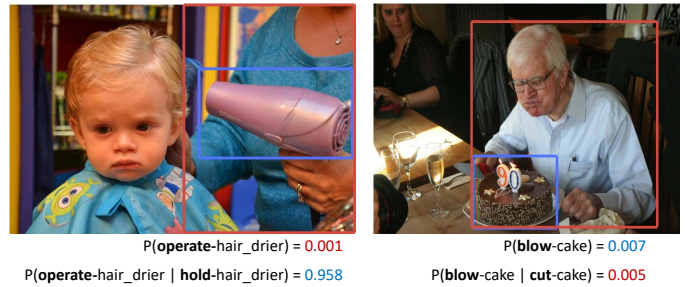


Fig. 1. Examples of action co-occurrence in HOI detection datasets. The marginal/conditional probability values are computed from the distribution of training labels. Intuitively, detection of rarely labeled HOIs (operate-hair dryer) can be facilitated by detection of commonly co-occurring HOIs (hold-hair dryer). Also, non-detection of rare HOIs (blow-cake) can be aided by detection of incompatible HOIs (cut-cake). We leverage this intuition as a prior to learn an HOI detector effective on long-tailed datasets.

multiple actions or interactions can happen at the same time. For example, the HOI of ‘operate-hair dryer’ is rarely labeled and consequently hard to detect in the left image of Fig. 1. However, ‘operate-hair dryer’ often occurs when the more commonly labeled HOI of ‘hold-hair dryer’ is present. As a result, detection of ‘operate-hair dryer’ can be facilitated by detection of ‘hold-hair dryer’ in an image. On the other hand, the detection of an HOI may preclude other incompatible HOIs, such as for ‘cut-cake’ and ‘blow-cake’ in the right image of Fig. 1.

In this paper, we introduce the new concept of utilizing co-occurring actions as prior knowledge, termed as action co-occurrence priors (ACPs), to train an HOI detector. In particular, we count the co-occurrences of class labels present in the training data and leverage this knowledge to effectively train our model. In contrast to language-based prior knowledge which requires external data sources [34], [53], [92], co-occurrence priors can be easily obtained from the label statistics of the target dataset. We also propose two novel ways to exploit them. First, we design a neural network with hierarchical structure where the classification is initially performed with respect to *action groups*. Each action group is defined by one anchor action, where the anchor actions are mutually exclusive according to the co-occurrence prior. Then, our model predicts the fine-grained HOI class within the action group. With this approach, higher performance is attained by learning dedicated classifiers for distinguishing closely-related actions within a group. Second, we present a technique that employs knowledge distillation [24] to expand HOI labels so they can have more positive labels for potentially co-occurring

actions. During training, the predictions are regularized by the refined objectives to improve robustness, especially for rare classes. To the best of our knowledge, this is the first work to leverage label co-occurrences in HOI detection to alleviate the long-tailed distribution problem.

The main contributions of this work can be summarized as: (1) The novel concept of explicitly leveraging correlations among HOI labels to address the problem of long-tailed distributions in HOI detection; (2) Two orthogonal ways to leverage action co-occurrence priors, namely through a proposed hierarchical architecture and HOI label expansion via knowledge distillation. The resulting model is shown to be consistently advantageous in relation to state-of-the-art techniques on both the HICO-Det [3] and V-COCO [20] benchmark datasets.

This work is an extension of our previous conference paper [37]. The primary differences are as follows: (1) We extend our architecture to incorporate a self-attention module, whose purpose is to enrich the semantic content of each human-object pair by accounting for surrounding human-object pairs. In this way, global image context is leveraged to better understand the interaction of a human and object. (2) We additionally exploit linguistic prior knowledge through a word embedding regression loss for object classes. In the word embedding, object categories that are more semantically similar are closer together. With this loss, learning for rare HOI labels can benefit from more common HOI labels that are semantically similar, further alleviating dataset bias. This extended method including both of the new components is called ACP++. We show that ACP++ outperforms our previous ACP in all the application scenarios we demonstrate. In addition, we expand our experimental results and analysis to show multiple aspects of our proposed method’s algorithmic behavior.

## II. RELATED WORK

The HOI detection task is rooted in visual relationship detection (VRD) and scene graph generation. In this section, we summarize the recent work on HOI detection, VRD, and scene graph generation. We also review works that utilize a label hierarchy in multi-label learning.

**Human-Object Interaction** Human-Object Interaction was originally studied in the context of recognizing the function or ‘affordance’ of objects [7], [15], [17], [19], [65]. Early works focus on learning more discriminative features combined with variants of SVM classifiers [8], [9], [86], and leverage the relationship with human poses for better representation [8], [9], [88] or mutual context modeling [87].

Recently, a completely data-driven approach based on convolutional neural networks (CNNs) has brought dramatic progress to HOI. Many of the pioneering works constructed large-scale image datasets [3], [4], [20], [101] to set new benchmarks in this field. Since then, significant progress has been achieved in using CNNs for this problem [1], [3], [14], [13], [16], [22], [27], [31], [47], [48], [50], [62], [64], [71], [73], [76], [80], [81], [98].

Most of these works follow a two-step scheme of CNN feature extraction and multi-information fusion, where the multiple information may include human and object appearance [3], [14], [16], [62]; box relation (either box configuration

or spatial map) [1], [3], [16], [22], [81]; object category [1], [13], [22], [59]; human pose [22], [47], [48]; and particularly, linguistic prior knowledge [13], [31], [59]. More recent works tend to combine these various cues [22], [48], [73], [80]. These works differ from one another mainly in their techniques for exploiting external knowledge priors. Kato *et al.* [31] incorporate information from WordNet [55] using a Graph Convolutional Network (GCN) [39] and learn to compose new HOIs. Xu *et al.* [81] also use a GCN to model the general dependencies among actions and object categories by leveraging a VRD dataset [53]. Li *et al.* [48] utilize interactiveness knowledge learned across multiple HOI datasets. Peyre *et al.* [59] transfer knowledge from triplets seen at training to new unseen triplets at test time by analogy reasoning.

Different from the previous works that focus on network architecture and human representation, we propose an orthogonal perspective to reformulate the target action label space and corresponding loss function by leveraging *co-occurrence* relationships among action classes for HOI detection. To the best of our knowledge, this is the first work that leverages the co-occurrence relationship between actions for HOI recognition. In principle, our method is complementary to all of the previous works and can be combined with any of them. We have implemented our approach on several existing HOI detection architectures [13], [22], [50], and we mainly evaluated our method with a baseline presented in [22] with details described in Sec. III-C.

**Visual Relationship Detection and Scene Graph Generation** The closest problems to HOI detection are Visual Relationship Detection (VRD) [6], [44], [60], [85], [91], [92], [94], [95], [97], [100] and scene graph generation [45], [18], [46], [79], [61], [77], [82], [84], [93], which deal with general visual relationships between two arbitrary objects. In VRD and scene graph datasets [40], [53], the types of visual relationships that are modeled include verb (action), preposition, spatial and comparative phrase. Scene graph generation, VRD, and HOI detection share common challenges such as long-tailed distributions and even zero-shot problems [53]. In this paper, we focus on HOI detection, as co-occurrences of human-object interactions are often strong, but the proposed technique could be extended to model the general co-occurrences that exist in visual relationships. While several other works on different tasks explore co-occurrence or contextual relation implicitly [12], [41], [42], [43], [56], [66], [69], [72], [89], [90], we explicitly model the co-occurrence of the data so that we can more efficiently exploit co-occurrence priors. In addition, as mentioned before, our method is complementary to the existing scene graph generation methods.

**Label Hierarchy in Multi-label Learning** The hierarchical structure of label categories has long been exploited for multi-label learning in various vision tasks, *e.g.*, image/object classification [10], [83], detection [29], [54], and human pose estimation [67], [68]. In contrast, label hierarchy has rarely been considered in HOI detection. Inspired by previous work [10] that uses Hierarchy and Exclusion (HEX) graphs to encode flexible relations between object labels, we introduce the first method to take advantage of an action label hierarchy for HOI recognition. While label hierarchies have

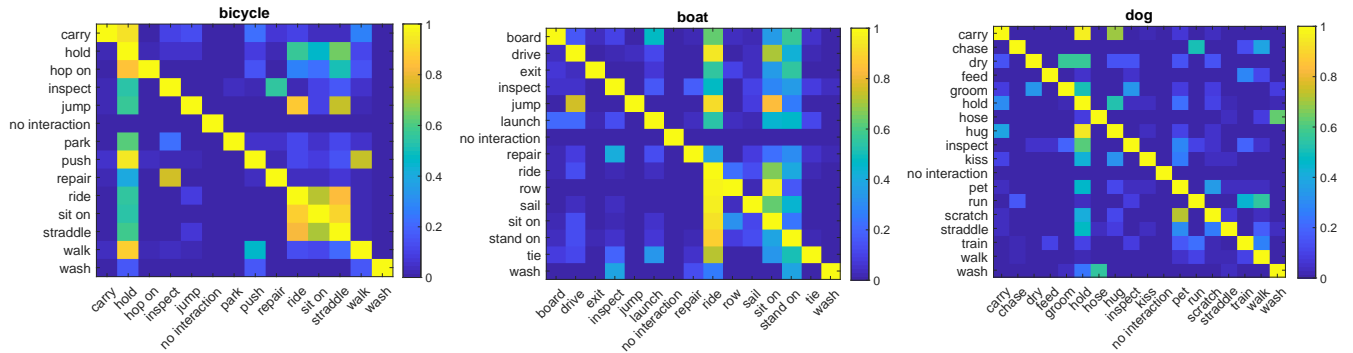


Fig. 2. Examples of co-occurrence matrices constructed for several objects (bicycle, boat, dog). Along the Y-axis is the given action, and the X-axis enumerates conditional actions. Each element represents the conditional probability that an action occurs when another action is happening.

commonly been used, our method is different in that it is defined by co-occurrences (rather than privileged semantics or a taxonomy [10]). This co-occurrence based hierarchy can be determined statistically, without direct human supervision.

### III. PROPOSED METHOD

Our method for utilizing the co-occurrence information of HOI labels consists of three key components: (1) establishing action co-occurrence priors (Sec. III-A), (2) hierarchical learning including anchor action selection (Sec. III-B) and devising the hierarchical architecture (Sec. III-C), followed by an extension of the architecture via self-attention (Sec. III-D), and (3) ACP projection for knowledge distillation (Sec. III-E), followed by an extension of the loss function via a language prior (Sec. III-F).

#### A. Action Co-occurrence Priors

Here, we formalize the action co-occurrence priors. The priors for the actions are modeled by a co-occurrence matrix  $C \in \mathbb{R}^{N \times N}$  where an entry  $c_{ij}$  in  $C$  represents the conditional probability that action  $j$  occurs when action  $i$  is happening:

$$c_{ij} = p(j|i), i, j \in [0, N), \quad (1)$$

where  $N$  (117 for the HICO-Det [3] dataset) denotes the total number of action classes and  $i, j$  are indices of two actions. By definition, the diagonal entries are one.  $C$  is constructed from the target HOI detection dataset by counting the image-level statistics of its training labels. Examples of co-occurrence matrices constructed for a single object are visualized in Fig. 2.

Meanwhile, we also consider the complementary event of action  $i$  (i.e., where the  $i$ -th action does not occur) and denote it as  $i'$ , such that  $p(i') + p(i) = 1$ . The complementary action co-occurrence matrix  $C' \in \mathbb{R}^{N \times N}$  can thus be defined by entries  $c'_{ij}$  in  $C'$  that represent the conditional probability that an action  $j$  occurs when another action  $i$  does not occur:

$$c'_{ij} = p(j|i'), i, j \in [0, N). \quad (2)$$

In this matrix, the diagonal entries are zero.

It can be seen from Fig. 2 that different types of relationships can exist between actions. They can be divided into three forms. The first is the **prerequisite** relationship, where the given action is highly likely to co-occur with

the conditional action. For example, the HOI ‘sit on-bicycle’ is a prerequisite of the HOI ‘ride-bicycle’. In this case,  $p(\text{sit on-bicycle}|\text{ride-bicycle})$  is close to 1. Next is **exclusion**, where the given action is highly unlikely to co-occur with the conditional action. An example is that the HOI ‘wash-bicycle’ and HOI ‘ride-bicycle’ are unlikely to happen together. As a result,  $p(\text{wash-bicycle}|\text{ride bicycle})$  is close to 0. Finally, we have **overlapping**, where the given action and conditional action may possibly co-occur, for example HOI ‘hold-bicycle’ and HOI ‘inspect-bicycle’, such that  $p(\text{hold-bicycle}|\text{inspect-bicycle})$  is in between 0 and 1. We introduce two ways to exploit the co-occurrence matrix by regarding exclusion (action space partitioning) and prerequisite actions (knowledge distillation). Detailed descriptions of the proposed methods are presented in the following sections.

The strong relationships that may exist between action labels can provide strong priors on the presence or absence of an HOI in an image. In contrast to previous works where models may implicitly learn label co-occurrence via relational architectures [2], [96], we explicitly exploit these relationships between action labels as priors, to effectively train our model especially for rare HOIs.

#### B. Anchor Action Selection via Non-Exclusive Suppression

From a co-occurrence matrix for an object, one can see that some actions are close in semantics or commonly co-occur while others are not. Intuitively, visually similar actions (e.g., ‘ride-horse’ and ‘hop on-horse’) tend to be harder to distinguish from each other, but these actions should not occur at the same time. If the positive labels for these actions are rare, then they become even more difficult to distinguish. Such cases require fine-grained recognition [11] and demand more dedicated classifiers. This motivates us to learn HOI classes in a coarse-to-fine manner. In particular, as a pre-processing step, we first collect a set of mutually exclusive action classes, called *anchor actions*, which tend to be distinguishable from one another. The anchor actions are used to partition the entire action label space into fine-grained sub-spaces. The other action classes are attributed to one or more sub-spaces and recognized in the context of a specific anchor action. In summary, unlike previous HOI detection works which predict action probabilities independently of one another, we divide the whole action label set into two sets, one for anchor actions

and one for regular actions, which are modeled in different ways as explained in detail in Sec. III-C.

Before training, in selecting anchor actions, we seek a set of action classes that are exclusive of one another. To this end, we define the exclusiveness of an action class as counting the number of actions that never occur if action  $i$  is happening:

$$e_i = \sum_j (1 \text{ if } (c_{ij} = 0), \text{ else } 0). \quad (3)$$

$e_i$  will have a high value if few other actions can occur when  $i$  does. Based on exclusiveness values, the anchor action label set  $\mathcal{D}$  is generated through *non-exclusive suppression (NES)* as described in Alg. 1. It iteratively finds the most exclusive action class as an anchor action and removes remaining action classes that are not exclusive to the selected anchor actions. The anchors in the list are action classes that never occur together in the training labels. For example, if an action such as ‘toast’ is on the anchor list, then actions like ‘stand’ and ‘sit’ cannot be on the list because they may co-occur with ‘toast’, while actions such as ‘hunt’ or ‘hop on’ can potentially be on the list. While there may exist other ways the anchor action selection could be done, we empirically found this approach to be simple, effective in terms of detection accuracy, and computationally efficient (less than 0.01 second).

---

**Algorithm 1:** Non-Exclusive Suppression (NES) algorithm for mutually exclusive anchor action selection.

---

**Input:**  $\mathcal{E} = \{e_i, i \in [0, N]\}, \mathcal{C} = \{c_{ij}, i, j \in [0, N]\};$   
**Output:**  $\mathcal{D}$

```

begin
   $\mathcal{D} \leftarrow \{\};$ 
  while  $\mathcal{E}$  is not empty do
    # Find the most exclusive action;
     $m \leftarrow \operatorname{argmax} \mathcal{E};$ 
     $\mathcal{D} \leftarrow \mathcal{D} \cup \{m\};$ 
    for  $e_k \in \mathcal{E}$  do
      # Remove the actions correlated (not
      exclusive) to  $m$ ;
      if  $c_{mk} > 0$  then
        |  $\mathcal{E} \leftarrow \mathcal{E} - e_k; \mathcal{C} \leftarrow \mathcal{C} - \{c_{ij}, i \text{ or } j = k\}$ 
      end
    end
  end
end
end

```

---

The anchor action label set acts as a finite partition of the action label space (a set of pairwise disjoint events whose union is the entire action label space). To form a complete action label space, we add an ‘*other*’ anchor action, denoted as  $\mathcal{O}$ , for when an action class does not belong to  $\mathcal{D}$ . Finally, we have  $|\mathcal{D}| + 1$  anchor actions including  $\mathcal{D}$  and the ‘*other*’ action class  $\mathcal{O}$ .

There are several benefits to having this anchor action label set. First, only one anchor action can happen at one time between a given human and object. Thus, we can use the relative (one-hot) probability representation with *softmax* activation instead of a sigmoid, where softmax features were

shown to compare well against distance metric learning-based features [26]. Second, anchor actions tend to be easier to distinguish from one another since they generally have prominent differences in an image. Third, it decomposes the action label space into several sub-spaces, which facilitates a coarse-to-fine solution. Each sub-task will have a much smaller solution space, which can improve learning. Finally, each sub-task will use a standalone sub-network which focuses on image features specific to the sub-task, which is an effective strategy for fine-grained recognition [11].

After selecting anchor actions, the entire action label set  $\mathcal{A}$  is divided into the anchor action label set  $\mathcal{D}$  and the remaining set of ‘regular’ action classes  $\mathcal{R}$ , so that  $\mathcal{A} = \{\mathcal{D}, \mathcal{R}\}$ . Each of the regular action classes is then associated with one or more anchor actions to form  $|\mathcal{D}| + 1$  action groups  $\mathbf{G} = \{\mathcal{G}_i; i \in \mathcal{D} \cup \mathcal{O}\}$ , one for each anchor action. A regular action class  $j \in \mathcal{R}$  will be assigned to the group associated with anchor action  $i$  ( $\mathcal{G}_i$ ) if action  $j$  is able to co-occur with the anchor action  $i$ ,

$$j \in \mathcal{G}_i, \text{ if } c_{ij} > 0 \quad (i \in \mathcal{D} \cup \mathcal{O}, j \in \mathcal{R}). \quad (4)$$

Note that the anchor actions themselves are not included in the action groups and a regular action  $j$  can be assigned to multiple action groups since it may co-occur with multiple anchor actions.

### C. Hierarchical Architecture

We implement our hierarchical approach upon several existing HOI detection architectures [13], [22], [50]. In this section, we introduce our main baseline architecture, built on the ‘No-Frills’ (NFs) baseline presented in [22] on account of its simplicity, effectiveness, and code availability [21]. Here, we give a brief review of the NFs architecture.

**Baseline Network** NFs follows the common scheme of CNN feature extraction followed by multi-information fusion. The feature extraction uses an off-the-shelf Faster R-CNN [63] object detector with ResNet152 [23] backbone network to detect human and object bounding boxes. From the final fully connected (FC) layer of the detector, the features  $\hat{x} = \{\hat{x}_h, \hat{x}_o\}$  are extracted, where  $\hat{x}_h$  and  $\hat{x}_o$  denote human and object appearance, respectively. These CNN features, together with the human pose ( $\hat{k}$ ), object category ( $\hat{o}$ ) and bounding boxes ( $\hat{b}$  including both object and human bounding boxes) compose the multiple information as  $X = \{\hat{x}, \hat{k}, \hat{o}, \hat{b}\}$ . As illustrated in Fig. 3, they are fed to our target model via corresponding network streams: human appearance ( $f_h$ ), object appearance ( $f_o$ ), bounding box and object category ( $f_b$ ), and human pose and object category ( $f_k$ ). Each individual type of information is first fed through a separate network of two FC layers to generate a fixed dimension (number of actions  $N$ ) feature. Then, all the features are added together and sent through a *sigmoid* activation to obtain the probability prediction for the action  $a$ :

$$\hat{A} = \operatorname{sigmoid}(F(X)) \in \mathbb{R}^N, \quad (5)$$

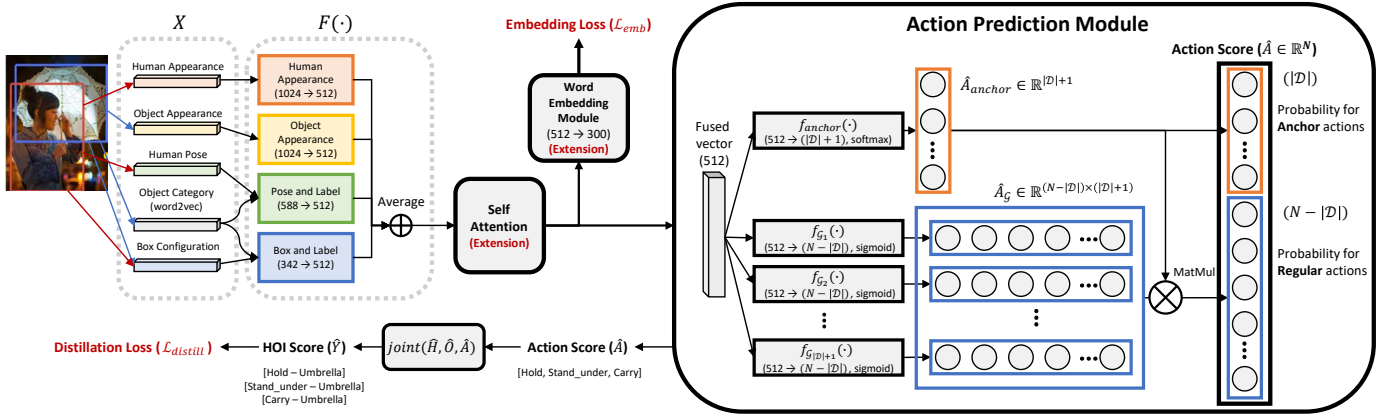


Fig. 3. Illustration of our overall network architecture. Our work differs from the baseline [22] by the addition of a hierarchical *action prediction module*. For our hierarchical architecture, anchor action probabilities are directly generated by a *softmax* sub-network. Regular action probabilities are generated by a matrix multiplication of the anchor probability and the output from a few *sigmoid* based conditional sub-networks.

where  $\hat{A}(a) = p(a|X)$  represents the probability prediction for action class  $a$ . The multi-information fusion procedure  $F(X)$  is expressed as

$$F(X) = f_h(\hat{x}_h) + f_o(\hat{x}_o) + f_k(\hat{k}||\hat{o}) + f_b(\hat{b}||\hat{o}), \quad (6)$$

where  $||$  denotes concatenation. The baselines built on other models [13], [50] are constructed in a similar manner.

To eliminate training-inference mismatch, NFs directly optimizes the HOI class probabilities instead of separating the detection and interaction losses as done in [14], [16]. The final HOI prediction is a joint probability distribution over  $M$  number of HOI classes (600 for HICO-Det dataset) computed from the probabilities  $\hat{H}$ ,  $\hat{O}$ , and  $\hat{A}$  for human, object, and action, respectively:

$$\hat{Y} = joint(\hat{H}, \hat{O}, \hat{A}) \in \mathbb{R}^M. \quad (7)$$

Specifically, for an HOI class  $(h, o, a)$ ,

$$\hat{Y}(h, o, a) = \hat{H}(h) * \hat{O}(o) * \hat{A}(a) = p(h|I) * p(o|I) * p(a|X), \quad (8)$$

where  $\hat{H}(h) = p(h|I)$  and  $\hat{O}(o) = p(o|I)$  are the probability of a candidate box pair being a human  $h$  and object  $o$ , provided by the object detector [63]. Finally, the binary cross-entropy loss  $\mathcal{L}(\hat{Y}, Y^{gt})$  is directly computed from the HOI prediction. This ‘No-Frills’ baseline network is referred to as **Baseline**.

**Modified Baseline Network** For a stronger baseline comparison, we make two simple but very effective modifications on the baseline network. (1) Replace the one-hot representation with the Glove word2vec [58] representation for the object category ( $\hat{o}$ ). (2) Instead of directly adding up the multiple information, we average them and forward this through another *action prediction module* to obtain the final action probability prediction. As a naive implementation of the **Modified Baseline**, we simply use a sub-network  $f_{sub}$  of a few FC layers as the *action prediction module*. Then Eq. (5)-6 are modified to

$$\hat{A} = sigmoid(f_{sub}(F(X))), \quad (9)$$

$$F(X) = \frac{f_h(\hat{x}_h) + f_o(\hat{x}_o) + f_k(\hat{k}||\hat{o}) + f_b(\hat{b}||\hat{o})}{n_{stream}}. \quad (10)$$

In this case,  $n_{stream} = 4$ .

Our hierarchical architecture further modifies the *action prediction module* by explicitly exploiting ACP information as described in the next paragraph.

**Proposed Hierarchical Architecture** Now we introduce the *action prediction module* for our hierarchical architecture (illustrated in Fig. 3) that better exploits the inherent co-occurrence among actions. While the baseline network predicts all the action probabilities directly from  $F(\cdot)$  with a single feed-forward sub-network  $f_{sub}$ , we instead use  $|\mathcal{D}| + 2$  sub-networks where one ( $f_{anchor}(\cdot)$ ) is first applied to predict the anchor action set and then one of the  $|\mathcal{D}| + 1$  other sub-networks ( $f_{G_i}(\cdot)$ ) which corresponds to the predicted anchor action is used to estimate the specific action within the action group. Because of the mutually exclusive property of anchor actions, we use the *softmax* activation for anchor action predictions, while employing the *sigmoid* activation for regular action prediction conditioned on the action group:

$$\hat{A}_{anchor} = softmax(f_{anchor}(F(X))) \in \mathbb{R}^{|\mathcal{D}|+1} \quad (11)$$

$$\hat{A}_{G_i} = sigmoid(f_{G_i}(F(X))) \in \mathbb{R}^{N-|\mathcal{D}|}, \text{ where } i \in \mathcal{D} \cup \mathcal{O}, \quad (12)$$

where  $\hat{A}_{anchor}(i)$  is directly used as the final probability predictions for the anchor actions:

$$p(i|X) = \hat{A}_{anchor}(i), i \in \mathcal{D}. \quad (13)$$

We let  $\hat{A}_{G_i}(j)$  represent the learned conditional probability that action  $j$  occurs when action  $i$  is happening, namely,

$$\hat{A}_{G_i}(j) = p(j|i, X). \quad (14)$$

Since the anchor action set is a finite partition of the entire action label space, the probability of a regular action  $j$  is predicted according to the law of total probability:

$$\begin{aligned} \hat{A}_{regular}(j) &= p(j|X) = \sum_{i \in \mathcal{D} \cup \mathcal{O}} p(i|X) * p(j|i, X) \\ &= \sum_{i \in \mathcal{D} \cup \mathcal{O}} \hat{A}_{anchor}(i) * \hat{A}_{G_i}(j), \end{aligned} \quad (15)$$

where  $j \in \mathcal{R}$ . Thus, instead of Eq. (9), we obtain the final action probability predictions for our hierarchical architecture  $\hat{A}(a) = p(a|X)$  as

$$\hat{A}(a) = \begin{cases} \hat{A}_{anchor}(a), & \text{if } a \in \mathcal{D} \\ \sum_{i \in \mathcal{D} \cup \mathcal{O}} \hat{A}_{anchor}(i) * \hat{A}_{\mathcal{G}_i}(a), & \text{otherwise.} \end{cases} \quad (16)$$

We use the same method as in Eq. (8) and a cross-entropy loss  $\mathcal{L}$  to compute the final HOI probability prediction  $\hat{Y}$ .

To demonstrate the effectiveness of the hierarchical learning, we introduce two other baselines, **MultiTask** and **TwoStream**, that lie between the **Modified Baseline** and our hierarchical learning. **MultiTask** only uses the anchor action classification as an additional multi-task element to the **Modified Baseline**. **TwoStream** separately predicts the anchor and the regular actions but without using the hierarchical modeling between anchor and regular actions.

#### D. Self-Attention Module Extension

In order to enhance the capability for holistic relational understanding across objects or humans, we additionally leverage a self-attention module that applies the non-local layer [78] to each human-object pair. In particular, let  $Z \in \mathbb{R}^{B \times 512}$  denote a stack of  $B$  merged human-object features from our  $F(\cdot)$  ( $Z = F(X)$ ). Then, we compute the relational association matrix by:

$$R = \text{Softmax}(\sigma(ZW_a)\sigma(ZW_b)^\top) \in \mathbb{R}^{B \times B}, \quad (17)$$

where  $\sigma(\cdot)$  denotes ReLU and  $W_a, W_b \in \mathbb{R}^{512 \times 128}$  are learnable weights that map the human-object features  $Z$  to their own roles, (e.g., key and query) and the softmax operation is applied row-wise. Then, the relational feature matrix is computed by:

$$A = R\sigma(ZW_x)W_z^\top \in \mathbb{R}^{B \times 512}, \quad (18)$$

where  $W_x \in \mathbb{R}^{512 \times 128}$  and  $W_z \in \mathbb{R}^{512 \times 128}$  are again learnable weights. The matrix  $A$  encodes aggregated features across all the objects according to the degree of relational association given in  $R$ . This relational feature matrix is combined with the original feature  $Z$  by  $\tilde{Z} = Z + A$ , so that  $Z$  is enhanced by holistic relational information.

#### E. ACP Projection for Knowledge Distillation

Knowledge distillation [24] was originally proposed to transfer knowledge from a large network to a smaller one. Recently, knowledge distillation has been utilized for various purposes such as lifelong learning [49], multi-task learning [35] or modality transfer [5], [25]. Hu *et al.* [28] extended this concept to distill prior knowledge in the form of logic rules into a deep neural network. Specifically, they propose a teacher-student framework to project the network prediction (student) to a rule-regularized subspace (teacher), where the process is termed distillation. The network is then updated to balance between emulating the teacher's output and predicting the true labels.

Our work fits this setting as the ACPs can act as a prior to distill. We first introduce *ACP Projection* to map the action

distribution to the ACP constraints. Then, we use the teacher-student framework [28] to distill knowledge from ACPs.

**ACP Projection** In ACP Projection, an arbitrary action distribution  $A = \{p(i), i \in [0, N]\} \in \mathbb{R}^N$  is projected into the ACP-constrained probability space:

$$A^* = \text{project}(A, C, C') \in \mathbb{R}^N, \quad (19)$$

where  $A^*$  is the projected action prediction. The projected probability for the  $j$ -th action  $A^*(j) = p(j^*)$  is generated using the law of total probability:

$$\begin{aligned} p(j^*) &= \frac{1}{N} \sum_{i=1}^N (p(i) * p(j|i) + p(i') * p(j|i')) \\ &= \frac{1}{N} \left( \sum_{i=1}^N p(i) * c_{ij} + \sum_{i=1}^N (1 - p(i)) * c'_{ij} \right). \end{aligned} \quad (20)$$

In matrix form, the ACP projection is expressed as

$$\text{project}(A, C, C') = \frac{AC + (1 - A)C'}{N}. \quad (21)$$

In practice, we use the object-based action co-occurrence matrices  $C_o \in \mathbb{R}^{N \times N}$  and  $C'_o \in \mathbb{R}^{N \times N}$  which only count actions related to a specific object  $o$ . Fig. 2 shows examples of  $C_o$  with respect to object classes. Also, we give different weights  $\alpha$  and  $\beta$  as hyper-parameters to the action co-occurrence matrix  $C_o$  and its complementary matrix  $C'_o$ , with the weights subject to  $\alpha + \beta = 2, \alpha > \beta$ . The projection function is then modified to

$$\text{project}(A, C_o, C'_o) = \frac{\alpha AC_o + \beta(1 - A)C'_o}{N}. \quad (22)$$

This is done because we empirically found the co-occurrence relationships in  $C_o$  to generally be much stronger than the complementary actions in  $C'_o$ .

**Teacher-Student Framework** Now we can distill knowledge from the ACPs using ACP Projection in both the training and inference phases. There are three ways ACP Projection can be used: (1) Directly project the action prediction  $\hat{A}$  into the ACP-constrained probability space at the testing phase to obtain the final action output (denoted as **PostProcess**). (2) Project the action prediction  $\hat{A}$  in the training phase and use the projected action as an additional learning target [28], [92]. (3) Project the ground truth label  $H^{gt}, O^{gt}$ , and  $A^{gt}$  to the ACP space in the training phase and use the projected action  $\text{project}(A^{gt}, C_{O^{gt}}, C'_{O^{gt}})$  as an additional learning target. The second and third items are incorporated into the teacher-student framework as terms in a new objective function (denoted as **Distillation**):

$$\mathcal{L}_{distill} = \lambda_1 \mathcal{L}(\hat{Y}, Y^{gt}) + \lambda_2 \mathcal{L}(\hat{Y}, \hat{Y}_{projO}) + \lambda_3 \mathcal{L}(\hat{Y}, Y_{projO}^{gt}), \quad (23)$$

where

$$\hat{Y}_{projO} = \text{joint}(\hat{H}, \hat{O}, \text{project}(\hat{A}, C_{\hat{O}}, C'_{\hat{O}})) \in \mathbb{R}^M, \quad (24)$$

$$Y_{projO}^{gt} = \text{joint}(H^{gt}, O^{gt}, \text{project}(A^{gt}, C_{O^{gt}}, C'_{O^{gt}})) \in \mathbb{R}^M. \quad (25)$$

<sup>1</sup>The triplet ground truth labels  $H^{gt}, O^{gt}$ , and  $A^{gt}$  are straightforward to determine from the HOI ground truth label  $Y^{gt}$ .

$\lambda_1, \lambda_2, \lambda_3$  are balancing weights among the ground truth HOI term and the teacher objectives. The object type can be easily determined from the object probability predictions  $\hat{O}$  or the ground truth label  $O^{gt}$ . With the new objective function, rare classes receive different supervisions, so confusion between them can be alleviated.

### F. Word Embedding Loss Extension

As an extension to enhance performance, we add another loss term, namely a word embedding regression loss. Given a word2vec representation for the object category  $\hat{o}$ , we regress our model to the same object representation in the output by computing the regressed word embedding  $v$ . Similar to Peyre *et al.* [59], we design the word embedding regularization loss as the sigmoid loss function:

$$\mathcal{L}_{emb} = \sum_{i=1}^{|O|} 1_{(y^o=i)} \log\left(\frac{1}{1 + e^{-\hat{o} \cdot v}}\right), \quad (26)$$

where  $|O|$  is the number of objects (80 for HICO-Det datasets) and  $y^o \in \mathbb{R}^{|O|}$  is the class for the object. Multi-task learning with the object prediction works as prior knowledge for action prediction, which leads to performance improvements. Therefore, the total loss function can be described as a weighted sum of the knowledge distillation loss and the embedding loss:

$$\mathcal{L}_{total} = \mathcal{L}_{distill} + \lambda_0 \mathcal{L}_{emb}, \quad (27)$$

where  $\lambda_0$  is the additional balancing weight between Eq. (23) and Eq. (26). Note that, as we have an object word2vec vector as input, this word embedding regression loss can be seen as an auto-encoding loss which is commonly used as a regularizer.

## IV. EXPERIMENTS

The goal of the experiments is to show the effectiveness and generalizability of our method. In particular, we show that our method can consistently alleviate the long-tailed distribution problem in various setups by improving performance, especially for rare HOI classes. In this section, we describe the experimental setups and competing methods, and provide extensive performance evaluations and analysis of HOI detection with both quantitative and qualitative results.

### A. Datasets and Metrics

We evaluate the performance of our model on two popular HOI detection benchmark datasets, **HICO-Det** [3] and **V-COCO** [20]. HICO-Det [3] extends the HICO (Humans Interacting with Common Objects) dataset [4] which contains 600 human-object interaction categories for 80 objects. Different from the HICO dataset, HICO-Det additionally contains bounding box annotations for humans and objects of each HOI category. The vocabulary of objects matches the 80 categories of MS COCO [51], and there are 117 different verb (action) categories. The number of all possible triplets is  $117 \times 80$ , but the dataset contains positive examples for only 600 triplets. The training set of HICO-Det contains 38,118 images and 117,871 HOI annotations for 600 HOI classes. The test set has 9,658 images and 33,405 HOI instances.

TABLE I  
ABLATION STUDY ON THE HICO-DET DATASET. OUR FINAL MODEL (ACP++) THAT INCLUDES BOTH HIERARCHICAL ARCHITECTURE AND DISTILLATION FOLLOWED BY POST PROCESSING, ALONG WITH THE TWO TECHNICAL EXTENSIONS OF WORD EMBEDDING LOSS AND SELF-ATTENTION, SHOWS THE BEST PERFORMANCE AMONG THE BASELINES.

	Full	Rare	Non-rare
Baseline	17.56	13.23	18.85
Modified Baseline	19.09	13.09	20.89
+Hierarchical only	20.03	14.52	21.67
+Distillation only	19.98	13.67	21.86
+Hierarchical+Distillation	20.25	15.33	21.72
+Hierarchical+Distillation+Post (Ours, ACP)	<b>20.59</b>	<b>15.92</b>	<b>21.98</b>
+Hierarchical+Distillation+ $\mathcal{L}_{emb}$	20.76	<b>16.35</b>	22.08
+Hierarchical+Distillation+SA	20.89	14.43	22.81
+Hierarchical+Distillation+ $\mathcal{L}_{emb}$ +SA (ACP++)	20.96	15.12	22.70
+Hierarchical+Distillation+ $\mathcal{L}_{emb}$ +SA (ACP++) +Post	<b>21.27</b>	15.41	<b>23.02</b>

For evaluation, HICO-Det uses the mean average precision (mAP) metric. Here, an HOI detection is counted as a true positive if the minimum of the human overlap IOU and object overlap IOU with the ground truth is greater than 0.5. Following [3], HOI detection performance is reported for three different HOI category sets: (1) all 600 HOI categories (Full), (2) 138 categories with fewer than 10 training samples (Rare), and (3) the remaining 462 categories with more than 10 training samples (Non-rare). Two evaluation settings are examined: ‘Default’ and ‘Known Object’. For the ‘Known Object’ setting, we evaluate the detection only on the images containing the target object category (*e.g.*, “bike”) given the HOI class (*e.g.*, “riding-bike”).

V-COCO (Verbs in COCO) is a subset of MS-COCO [51], which consists of 10,346 images (2,533, 2,867, 4,946 for training, validation and test, respectively) and 16,199 human instances. Each person is annotated with binary labels for 26 action classes. For the evaluation metric, we use the AP score as done for the evaluation on HICO-Det.

### B. Quantitative Results

**Ablation study** In the ablations, the ‘No-Frills’ baseline network [22] we used is denoted as **Baseline**. We first evaluate the effectiveness of the core design components in the proposed method, including (1) our simple modification to **Baseline** in Sec. III-C, denoted as **Modified Baseline**; (2) the hierarchical learning technique introduced in Sec. III-C, denoted as **Hierarchical**; and (3) the knowledge distillation technique presented in Eq. (27) of Sec. III-E, denoted as **Distillation**. Moreover, we show additional baselines which include either the self-attention module from Sec. III-D (denoted as **SA**) or the word embedding loss function from Sec. III-F (denoted as  $\mathcal{L}_{emb}$ ).

TABLE II  
PERFORMANCE OF OUR MODELS WITH DIFFERENT ARCHITECTURES FOR ACTION PREDICTION MODULE. OUR MODEL ((D) HIERARCHICAL) SHOWS THE BEST PERFORMANCE AMONG THE DESIGN CHOICES.

	Full	Rare	Non-rare
(A) Modified Baseline	19.09	13.09	20.89
(B) MultiTask	19.54	13.93	21.22
(C) TwoStream	19.63	13.67	21.41
(D) Hierarchical	<b>20.03</b>	<b>14.52</b>	<b>21.67</b>

TABLE III

RESULTS ON THE HICO-DET DATASET COMPARED TO THE EXISTING STATE-OF-THE-ART METHODS. THE FIRST ROW SECTION SHOWS THE SCORES REPORTED IN THE PREVIOUS WORKS WHILE THE SECOND ROW SECTION SHOWS THE RESULTS OF OUR IMPLEMENTATIONS. THE PERFORMANCE OF OUR METHOD CONSISTENTLY SURPASSES THOSE OF THE EXISTING HOI DETECTORS.

	Default			Known Object		
	Full	Rare	Non-rare	Full	Rare	Non-rare
Shen <i>et al.</i> [64]	6.46	4.24	7.12	-	-	-
HO-RCNN [3]	7.81	5.37	8.54	10.41	8.94	10.85
Gupta <i>et al.</i> [20] impl. by [16]	9.09	7.02	9.71	-	-	-
InteractNet [16]	9.94	7.16	10.77	-	-	-
GPNN [62]	13.11	9.34	14.23	-	-	-
iCAN [14]	14.84	10.45	16.15	16.43	12.01	17.75
Interactiveness Prior [48]	17.22	13.51	18.32	19.17	15.51	20.26
Contextual Attention [75]	16.24	11.16	17.75	17.73	12.78	19.21
No-Frills [22]	17.18	12.17	18.68	-	-	-
RPNN [99]	17.35	12.78	18.71	-	-	-
PMFNet [73]	17.46	15.65	18.00	20.34	17.47	21.20
Peyre <i>et al.</i> [59]	19.40	15.40	20.75	-	-	-
PPDM [50]	21.10	14.46	23.09	-	-	-
DJ-RN [47]	21.34	18.53	22.18	23.69	20.64	24.60
FCMNet [52]	20.41	17.34	21.56	22.56	18.97	23.12
VCL [27]	19.43	16.55	20.29	22.00	19.09	22.87
DRG [13]	19.26	17.74	19.71	23.40	21.75	23.89
No-Frills (Reproduced)	17.56	13.23	18.85	22.02	16.97	23.53
No-Frills + <b>ACP (Ours)</b>	20.59	<b>15.92</b>	21.98	25.35	<b>19.55</b>	27.08
No-Frills + <b>ACP++ (Ours)</b>	<b>21.27</b>	15.41	<b>23.02</b>	<b>25.61</b>	18.93	<b>27.60</b>
PPDM (Reproduced)	20.81	13.69	22.94	-	-	-
PPDM + <b>ACP++ (Ours)</b>	<b>22.11</b>	<b>14.43</b>	<b>24.40</b>	-	-	-
DRG (Reproduced)	18.77	16.41	19.47	24.74	23.74	25.04
DRG + <b>ACP++ (Ours)</b>	<b>18.90</b>	<b>16.80</b>	<b>19.52</b>	<b>24.78</b>	<b>23.87</b>	<b>25.05</b>

TABLE IV

RESULTS ON THE V-COCO DATASET. FOR OUR METHOD, WE SHOW RESULTS BOTH FOR CONSTRUCTING ACP FROM V-COCO AND FOR USING ACP CONSTRUCTED FROM HICO-DET INSTEAD. BOTH OF THESE MODELS SHOW FAVORABLE PERFORMANCE AGAINST THE CURRENT STATE-OF-THE-ART MODELS.

	$AP_{role}$
Gupta <i>et al.</i> [20] impl. by [16]	31.8
InteractNet [16]	40.0
GPNN [62]	44.0
iCAN [14]	45.3
iHOI [80]	45.79
with Knowledge [81]	45.9
Interactiveness Prior [48]	48.7
Contextual Attention [75]	47.3
RPNN [99]	47.53
PMFNet [73]	52.0
VCL [27]	48.3
DRG [13]	51.0
VSGNet [71]	51.76
Interaction Points [76]	52.3
PD-Net [98]	52.6
Heterogeneous [74]	52.7
FCMNet [52]	53.1
UnionDet [32]	47.5
Our baseline	48.91
<b>ACP (Ours, V-COCO)</b>	<b>52.98</b>
<b>ACP (Ours, HICO-Det)</b>	<b>53.23</b>

Table I gives a comprehensive evaluation for each component. We draw conclusions from it one-by-one.

**First, our baseline network is strong.** Our *Modified Baseline* achieves 19.09 mAP and surpasses the ‘No-Frills’ *Baseline* by 1.51 mAP (a relative 8.7% improvement). This is already competitive to the state-of-the-art result [59] and serves as a strong baseline.

**Second, both hierarchical learning and knowledge distillation are effective.** This is concluded by adding *Hierarchical* and *Distillation* to the *Modified Baseline*, respectively. Specifically, **+Hierarchical** improves the modified baseline by 0.94 mAP (a relative 4.9% improvement), and **+Distillation** (training with Eq. (27)) improves the modified baseline by 0.89 mAP (a relative 4.7% improvement). Including both obtains 1.16 mAP improvement (relatively better by 6.1%).

**Third, the proposed ACP method achieves a new state-of-the-art.** Our final result is generated by further using the *PostProcess* step (introduced in Sec. III-E) that projects the final action prediction into the ACP constrained space. Our method achieves 20.59 mAP (relative 7.9% improvement) for Full HOI categories, 15.92 mAP (relative 21.6% improvement) for Rare HOI categories, and 21.98 mAP (relative 5.2% improvement) for Non-rare HOI categories. Note that our method made especially significant improvements for Rare classes, which supports the claim that the proposed method can alleviate the long-tailed distribution problem of HOI detection datasets. This result set the new state-of-the-art at the time of submission for our earlier version of this work [37] on both the HICO-Det and V-COCO datasets as shown in Table III and Table IV.

**Fourth, the extended ACP++ outperforms our previous ACP.** The word embedding loss ( $\mathcal{L}_{emb}$ ) improves the performance of our previous ACP model in all the metrics, especially on rare classes, by alleviating the bias in the dataset. In addition, self-attention module (SA) enhances the representation power of the model, thus it elevates the overall mAP by improving the performance on non-rare classes. However, SA reduces the performance on rare classes. We conjecture that the model overfits on the major classes due to the additional parameters introduced by the SA module and degrades the generalization ability on rare classes. Combining both of the technical extensions upon our previous ACP model gives the final extended ACP++ result. Without *PostProcess*, our extended method improves upon our original ACP method by 20.96 mAP (relative 3.5% improvement), and our extended method improves upon our original ACP method by 21.27 mAP (relative 3.3% improvement) with *PostProcess*.

In addition, the *MultiTask*, *TwoStream*, and our *Hierarchical* architecture are compared in Table II. From *MultiTask*, it can be seen that the *softmax* based anchor action classification already brings benefits to the *Modified Baseline* when used only in a multi-task learning manner. From *TwoStream*, separately modeling the anchor and the regular classes leads to slightly more improvement compared to *MultiTask*. Moreover, our *Hierarchical* architecture improves upon *TwoStream* by explicitly modeling the hierarchy between anchor and regular action predictions.

**Comparison with the state-of-the-art** We compare our method with the previous state-of-the-art techniques in Table III. The first and second column sections in Table III are for



TABLE V

COMPARISON OF OUR MODEL TO THE FUNCTIONAL GENERALIZATION METHOD OF BANSAL *et al.* [1]. THE TOP SET OF ROWS SHOWS THE SCORES OF THE BASELINE AND THE FUNCTIONAL GENERALIZATION MODEL WITHOUT TUNING AS REPORTED IN [1]. IN BOTTOM SET OF ROWS, WE SHOW THE RESULTS OF OUR IMPLEMENTATIONS THAT INCLUDE THE FUNCTIONAL GENERALIZATION MODEL AND OUR ACP METHOD. THE ACP METHOD CAN ACHIEVE LARGER PERFORMANCE GAINS THAN FUNCTIONAL GENERALIZATION.

	Full	Rare	Non-rare
Baseline of [1]	12.72	7.57	14.26
Functional Generalization [1]	14.35	9.84	15.69
Baseline of [1] (Reproduced)	13.09	7.87	14.65
Functional Generalization (Reproduced)	13.68	8.62	15.19
Functional Generalization + ACP (Ours)	<b>15.38</b>	<b>10.30</b>	<b>16.90</b>

‘Default’ and ‘Known Object’ matrices, respectively. Among the methods included in this comparison are the benchmark model of the HICO-Det dataset [3], the baseline models that we trained or modified from [13], [22], [50], and the current published state-of-the-art methods. As shown in Table III, our ACP model (Ours) shows consistent improvements over our baseline models on all metrics, with especially significant gains over the ‘No-Frills’ baseline, and shows favorable performance against the current state-of-the-art models in terms of all the metrics. In particular, our model (No-Frills + ACP++) surpasses the state-of-the-art model at the time of submission [59] by 1.87 mAP. We also added the result of applying ACP++ priors to more recent HOI detection methods [13], [50], and this also achieves consistent performance improvements for all the metrics. Note that ‘PPDM + ACP++’ model outperforms the state-of-the-art model without elaborate fine-tuning [47].

**Results on V-COCO dataset** To show the generalization ability of our method, we also evaluate it on the V-COCO dataset. Note that the exact same method is directly applied to both HICO-Det and V-COCO, including the co-occurrence matrix, anchor action selection, and architecture design. We also constructed a co-occurrence matrix from V-COCO, but the matrix was sparse. Thus, to better take advantage of our idea, we instead use the co-occurrence matrix collected from the HICO-Det dataset to train on V-COCO. Table IV shows the performance of our model implemented upon the ‘No-Frills’ model (Ours, HICO-Det) compared to the recent state-of-the-art HOI detectors on the V-COCO dataset. In addition, we show results of our model with the co-occurrence matrix constructed from the V-COCO dataset (Ours, V-COCO). Both of these models show favorable performance on the V-COCO dataset against the existing state-of-the-art models [52].

**Experiments with Functional Generalization [1]** We also examine our approach together with an HOI detection method called ‘Functional Generalization’ [1]. Since its paper does not provide the details for its elaborate fine-tuning (which led to improvements from 14.35 mAP to 21.96 mAP), we consider it to be unsuitable for comparison in Table III. However, we found our method to be complementary to its untuned version. As shown in Table V, according to our implementation, the functional generalization approach improves upon its baseline by 0.59 mAP (a relative 4.51% improvement), while adding

TABLE VI

RESULTS ON THE ZERO-SHOT TRIPLETS OF THE HICO-DET DATASET. OUR FINAL MODEL SHOWS BETTER PERFORMANCE THAN PEYRE *et al.* BY A LARGE MARGIN. OUR ACP MODEL UNDER THE ZERO-SHOT SETTING EVEN OUTPERFORMS THE SUPERVISED SETTING OF OUR BASELINE.

	mAP
Peyre <i>et al.</i> [59] Supervised	33.7
Peyre <i>et al.</i> [59] Zero-Shot	24.1
Peyre <i>et al.</i> [59] Zero-Shot with Aggregation	28.6
Ours Supervised (Modified Baseline)	33.27
Ours Zero-Shot (Modified Baseline)	20.34
<b>Ours Zero-Shot (ACP)</b>	<b>34.95</b>
<b>Ours Zero-Shot (ACP++)</b>	<b>35.12</b>

our ACP method to the functional generalization model improves it by 1.70 mAP (a relative 12.43% improvement). This indicates that our ACP method can complement other methods such as Functional Generalization. In addition, the results suggest that the ACP method can achieve larger performance gains than Functional Generalization. Finally, note that the Functional Generalization method requires word vectors pre-trained on an external dataset, whereas our ACP prior can be constructed from only the labels of our target dataset.

**Results of the zero-shot setup on the HICO-Det dataset** The *zero-shot setting* on the HICO-Det dataset was defined by Peyre *et al.* [59]. Specifically, we select a set of 25 HOI classes that we treat as unseen classes and exclude them and their labels in the training phase. However, we still let the model predict those 25 unseen classes in the test phase, which is known as the zero-shot problem. These HOI classes are randomly selected from among the set of non-rare HOI classes. Since Peyre *et al.* did not provide which specific HOI classes they selected, we select the unseen HOI classes such that the performance (mAP) for these classes in our *Modified Baseline* model (introduced in Sec. III-C) is similar to the corresponding *Supervised* baseline in [59]. In Table VI, we show results of our final model (ACP and ACP++) and our modified baseline model compared to the corresponding setting reported in [59]. Our ACP model shows better performance (35.0 mAP) than Peyre *et al.* (28.6 mAP) by a large margin (relative 22.4% improvement). In addition, our extended model (ACP++) further improves the performance of our ACP (35.1 mAP). This result is remarkable in that our ACP model under the zero-shot setting even *outperforms* the supervised setting of our baseline model, indicating the power of the proposed ACP method to effectively leverage prior knowledge on action co-occurrences. Furthermore, the analogy transfer method proposed by Peyre *et al.* (denoted as aggregation) requires large-scale linguistic knowledge to train a word representation, whereas our model only requires the co-occurrence information of the labels in the dataset, which is much easier to obtain. We conclude that the proposed method is effective for the zero-shot problem while being easy to implement.

### C. Qualitative Results and Analysis

**Qualitative results** In addition, Fig. 4 shows examples of HOI detection results that our model predicts correctly with high probability. We show each image with the predicted HOI class

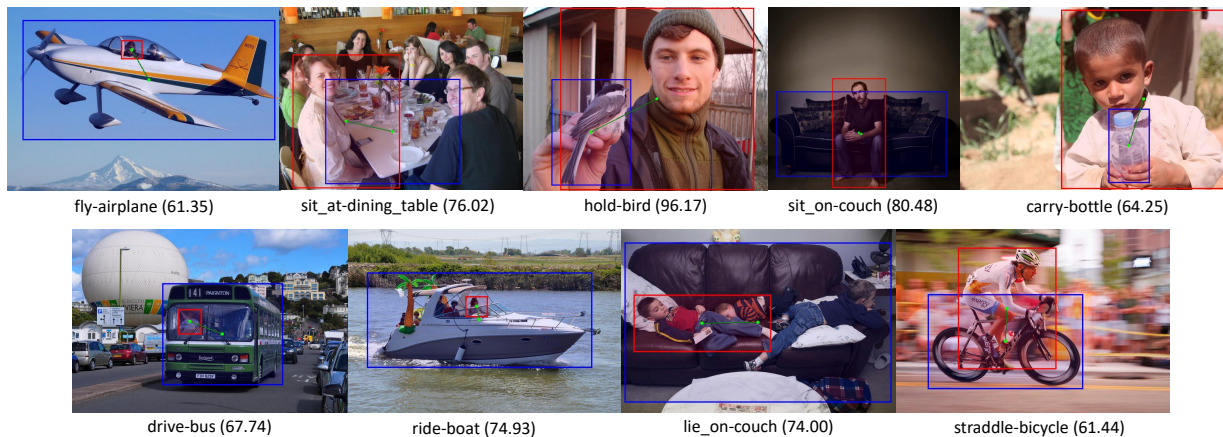


Fig. 4. Examples of bounding boxes and HOI detection scores from our model. Bounding boxes for humans are colored red, and bounding boxes for objects are colored blue. Each image is displayed with the predicted action+object class followed by the probability computed by our model.

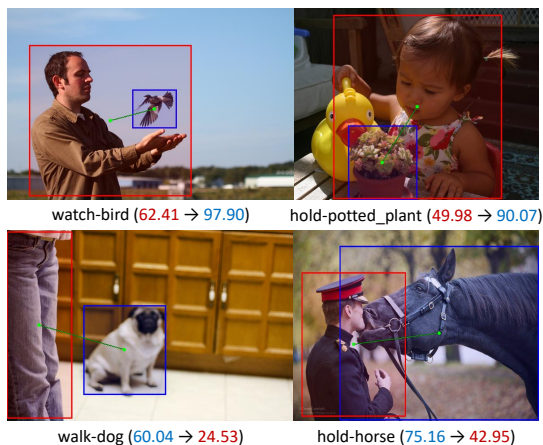


Fig. 5. The HOI probability before and after applying the projection function  $project(\cdot)$  on our model’s HOI prediction (*PostProcess*). Note that *PostProcess* can be done without any optimization.

followed by the probability computed by our model. Also, we show the HOI probability change from before to after applying the projection function  $project(\cdot)$  on our model’s HOI prediction (*i.e.*, the effect of *PostProcess* introduced in Sec. III-E) in Fig. 5. Leveraging co-occurrence matrix  $C$  not only increases the score for true classes (top) but also reduces the score for false classes (bottom). Note that this change can be achieved *without any optimization* process. Moreover, we show changes in HOI probability from before to after applying the self-attention in our model in Fig. 6. It is found that our self-attention module mostly reduces the probability for rare classes (even for true classes), which might be the reason for the mAP degradation on rare classes shown in Table I.

**Number of anchor actions** In addition, we investigate the effect of using different numbers of anchor actions  $|\mathcal{D}|$  in Fig. 7. We measure the relative performance improvement from the **+Hierarchical** model to the **Modified Baseline** model by changing the number of anchor actions at intervals of five.

In principle, the more anchor actions we use, the better performance that can be attained. On one hand, the selected anchor actions can be more distinguishable from one another with more anchor action categories and training samples. On the other hand, the remaining regular actions can also benefit

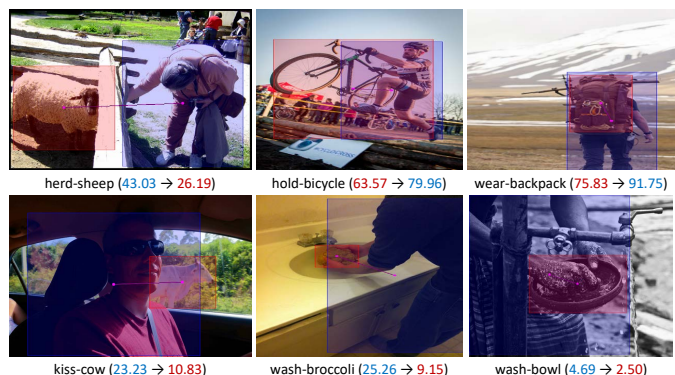


Fig. 6. The HOI probability before and after applying the self-attention in our model for non-rare (top row) and rare (bottom row) HOI classes. For non-rare classes, our self-attention increases the score for true classes (‘hold-bicycle’ and ‘wear-backpack’) and reduces the score for false classes (‘herd-sheep’). On the other hand, for rare classes, the self-attention mostly reduces the scores even for true classes (*e.g.*, ‘wash-bowl’ and ‘wash-broccoli’).

from stronger co-occurrence priors. However, more anchor action will also result in more sub-networks to optimize, and this will cause over-fitting to a certain extent. Through observations, we found that an increase in the number of parameters of the HOI detector often causes a severe performance decrease. Thus, there is a trade-off between a large and small number of anchors, which requires us to empirically select the best anchor number. As depicted in Fig. 7, the hierarchical architecture shows the best overall mAP score (Full) with 15 anchors and the best mAP score on rare classes with 10 anchors. We finally use an experimentally overall best-performing choice of 15 anchor actions (maximum anchor action number is 54).

**Performance on various sets with different number of training samples** In Fig. 8, we show the relative mAP score improvements of our model compared to the baseline model by computing mAP on various sets of HOI classes that have different number of training samples. Our method shows positive performance improvements for all numbers of training samples. Also, there is a trend that HOI classes with a small number of training samples mostly show larger performance improvements. In particular, for HOI classes with the number

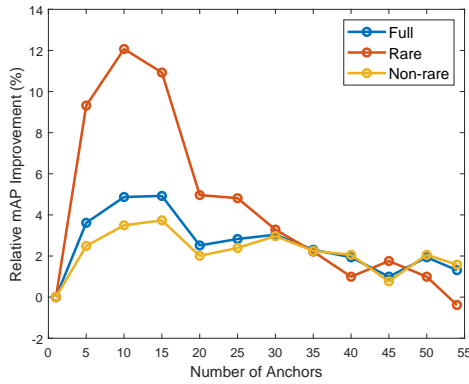


Fig. 7. Performance of the hierarchical architecture with different numbers of anchors at intervals of five. The models with 15 and 10 anchors show the best performance overall and on rare classes, respectively.

of training samples between 0 and 9, our model achieves 38.24% improvement compared to the baseline model. These results indicate that the proposed method is able to improve the performance of an HOI detector, especially for classes with few training samples.

**Analysis of false predictions** Fig. 9 shows examples of false predictions by our model. We found three common reasons for predictions being evaluated as false. First is the wrong prediction of object label from the object detector (*e.g.*, ‘couch’ as ‘chair’ or ‘sheep’ as ‘cow’) which is shown in the left column of Fig. 9. Second, the prediction is correct but the ground truth label for the prediction in a test image is missing (*e.g.*, ‘ride-bus’ or ‘hold-horse’) which is shown in the middle column of Fig. 9. Last, an HOI detector could have been predicted correctly if there were a sophisticated way to take context (the third object or the background) into account (*e.g.*, the background for predicting ‘repair-bicycle’ or an object that person carries for predicting ‘load-bus’) which is shown in the right column of Fig. 9. The last issue could be solved by devising a better network architecture for effectively encoding context, which is a direction orthogonal to our work. All of these issues (the errors in the object detector, missing labels in datasets, and encoding context) are fundamental issues in HOI detection, which can be interesting topics for future work.

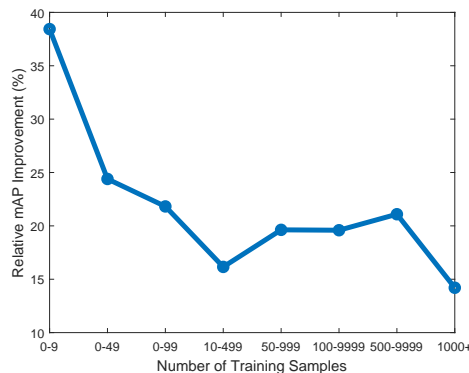


Fig. 8. The relative mAP score improvements for various HOI sets with different numbers of training samples. Our method is able to improve the performance especially when the number of training samples is small (38.24% improvement for 0-9 samples).

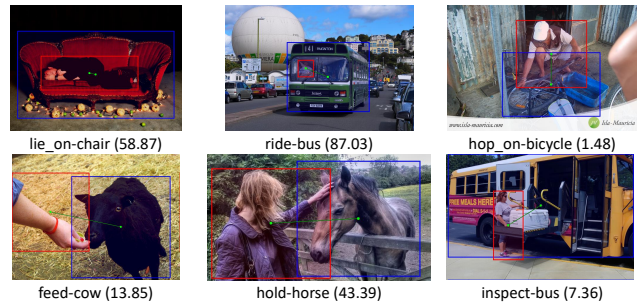


Fig. 9. Examples of the false predictions from our model. The false cases include wrong prediction of object label from the object detector (left column), correct prediction but missing ground truth labels (middle column), and predictions that could have been correct if the context were taken into account (right column).

V. CONCLUSION

We introduced a novel method to effectively train an HOI detector by leveraging prior knowledge on action co-occurrences in two different ways, via the architecture and via the loss function. Our proposed method consistently achieves favorable performance compared to the current state-of-the-art methods in various setups. Co-occurrence information not only is helpful for alleviating the long-tailed distribution problem but also can be easily obtained. Given the co-occurrence action/interaction priors, one open question is how to expand the co-occurrence priors to a larger vocabulary and more general domains. Therefore, a possible direction for future work would be obtaining more general co-occurrence priors by leveraging external knowledge from the web. Another direction for future work is to construct and utilize co-occurrence priors for other relationship-based vision tasks [30], [33], [36], [53] or other problems related to the dataset bias [38], [57], [70].

**Acknowledgements.** This work was supported by the Institute for Information & Communications Technology Promotion (2017-0-01772) grant funded by the Korea government.

REFERENCES

- [1] Ankan Bansal, Sai Saketh Rambhatla, Abhinav Shrivastava, and Rama Chellappa. Detecting human-object interactions via functional generalization. In *AAAI Conference on Artificial Intelligence (AAAI)*, 2020.
- [2] Fabien Baradel, Natalia Neverova, Christian Wolf, Julien Mille, and Greg Mori. Object level visual reasoning in videos. In *European Conference on Computer Vision (ECCV)*, 2018.
- [3] Yu-Wei Chao, Yunfan Liu, Xieyang Liu, Huayi Zeng, and Jia Deng. Learning to detect human-object interactions. In *IEEE Winter Conference on Applications of Computer Vision (WACV)*, 2018.
- [4] Yu-Wei Chao, Zhan Wang, Yugeng He, Jiaxuan Wang, and Jia Deng. Hico: A benchmark for recognizing human-object interactions in images. In *IEEE International Conference on Computer Vision (ICCV)*, 2015.
- [5] Jae Won Cho, Dong-Jin Kim, Jinsoo Choi, Yunjae Jung, and In So Kweon. Dealing with missing modalities in the visual question answer-difference prediction task through knowledge distillation. In *Proceedings of the IEEE/CVF Conference on Computer Vision and Pattern Recognition*, 2021.
- [6] Bo Dai, Yuqi Zhang, and Dahua Lin. Detecting visual relationships with deep relational networks. In *IEEE Conference on Computer Vision and Pattern Recognition (CVPR)*, 2017.

- [7] Vincent Delaitre, David F Fouhey, Ivan Laptev, Josef Sivic, Abhinav Gupta, and Alexei A Efros. Scene semantics from long-term observation of people. In *European Conference on Computer Vision (ECCV)*, 2012.
- [8] Vincent Delaitre, Ivan Laptev, and Josef Sivic. Recognizing human actions in still images: a study of bag-of-features and part-based representations. In *British Machine Vision Conference (BMVC)*, 2010.
- [9] Vincent Delaitre, Josef Sivic, and Ivan Laptev. Learning person-object interactions for action recognition in still images. In *Advances in Neural Information Processing Systems (NeurIPS)*, 2011.
- [10] Jia Deng, Nan Ding, Yangqing Jia, Andrea Frome, Kevin Murphy, Samy Bengio, Yuan Li, Hartmut Neven, and Hartwig Adam. Large-scale object classification using label relation graphs. In *European Conference on Computer Vision (ECCV)*, 2014.
- [11] Jianlong Fu, Heliang Zheng, and Tao Mei. Look closer to see better: Recurrent attention convolutional neural network for fine-grained image recognition. In *IEEE Conference on Computer Vision and Pattern Recognition (CVPR)*, 2017.
- [12] Carolina Galleguillos, Andrew Rabinovich, and Serge Belongie. Object categorization using co-occurrence, location and appearance. In *IEEE Conference on Computer Vision and Pattern Recognition (CVPR)*, 2008.
- [13] Chen Gao, Jiarui Xu, Yuliang Zou, and Jia-Bin Huang. Drg: Dual relation graph for human-object interaction detection. In *European Conference on Computer Vision (ECCV)*, 2020.
- [14] Chen Gao, Yuliang Zou, and Jia-Bin Huang. ican: Instance-centric attention network for human-object interaction detection. In *British Machine Vision Conference (BMVC)*, 2018.
- [15] James J Gibson. *The ecological approach to visual perception: classic edition*. Psychology Press, 2014.
- [16] Georgia Gkioxari, Ross Girshick, Piotr Dollár, and Kaiming He. Detecting and recognizing human-object interactions. In *IEEE Conference on Computer Vision and Pattern Recognition (CVPR)*, 2018.
- [17] Helmut Grabner, Juergen Gall, and Luc Van Gool. What makes a chair a chair? In *IEEE Conference on Computer Vision and Pattern Recognition (CVPR)*, 2011.
- [18] Jiuxiang Gu, Handong Zhao, Zhe Lin, Sheng Li, Jianfei Cai, and Mingyang Ling. Scene graph generation with external knowledge and image reconstruction. In *IEEE Conference on Computer Vision and Pattern Recognition (CVPR)*, 2019.
- [19] Abhinav Gupta and Larry S Davis. Objects in action: An approach for combining action understanding and object perception. In *IEEE Conference on Computer Vision and Pattern Recognition (CVPR)*, 2007.
- [20] Saurabh Gupta and Jitendra Malik. Visual semantic role labeling. *arXiv preprint arXiv:1505.04474*, 2015.
- [21] Tanmay Gupta, Alexander Schwing, and Derek Hoiem. No-Frills Pytorch Github. [https://github.com/BigRedT/no\\_frills\\_hoi\\_det](https://github.com/BigRedT/no_frills_hoi_det).
- [22] Tanmay Gupta, Alexander Schwing, and Derek Hoiem. No-frills human-object interaction detection: Factorization, layout encodings, and training techniques. In *IEEE International Conference on Computer Vision (ICCV)*, 2019.
- [23] Kaiming He, Xiangyu Zhang, Shaoqing Ren, and Jian Sun. Deep residual learning for image recognition. In *IEEE Conference on Computer Vision and Pattern Recognition (CVPR)*, 2016.
- [24] Geoffrey Hinton, Oriol Vinyals, and Jeff Dean. Distilling the knowledge in a neural network. *arXiv preprint arXiv:1503.02531*, 2015.
- [25] Judy Hoffman, Saurabh Gupta, and Trevor Darrell. Learning with side information through modality hallucination. In *IEEE Conference on Computer Vision and Pattern Recognition (CVPR)*, 2016.
- [26] Shota Horiguchi, Daiki Ikami, and Kiyoharu Aizawa. Significance of softmax-based features in comparison to distance metric learning-based features. *IEEE Transactions on Pattern Analysis and Machine Intelligence (TPAMI)*, 2019.
- [27] Zhi Hou, Xiaojiang Peng, Yu Qiao, and Dacheng Tao. Visual compositional learning for human-object interaction detection. In *European Conference on Computer Vision (ECCV)*, 2020.
- [28] Zhiting Hu, Xuezhe Ma, Zhengzhong Liu, Eduard Hovy, and Eric Xing. Harnessing deep neural networks with logic rules. In *Annual Meeting of the Association for Computational Linguistics (ACL)*, 2016.
- [29] Sung Ju Hwang, Fei Sha, and Kristen Grauman. Sharing features between objects and their attributes. In *IEEE Conference on Computer Vision and Pattern Recognition (CVPR)*, 2011.
- [30] Justin Johnson, Bharath Hariharan, Laurens van der Maaten, Li Fei-Fei, C Lawrence Zitnick, and Ross Girshick. Clevr: A diagnostic dataset for compositional language and elementary visual reasoning. In *IEEE Conference on Computer Vision and Pattern Recognition (CVPR)*, 2017.
- [31] Keizo Kato, Yin Li, and Abhinav Gupta. Compositional learning for human object interaction. In *European Conference on Computer Vision (ECCV)*, 2018.
- [32] Bumsoo Kim, Taeho Choi, Jaewoo Kang, and Hyunwoo J Kim. Union-det: Union-level detector towards real-time human-object interaction detection. In *European Conference on Computer Vision (ECCV)*, 2020.
- [33] Dong-Jin Kim, Jinsoo Choi, Tae-Hyun Oh, and In So Kweon. Dense relational captioning: Triple-stream networks for relationship-based captioning. In *IEEE Conference on Computer Vision and Pattern Recognition (CVPR)*, 2019.
- [34] Dong-Jin Kim, Jinsoo Choi, Tae-Hyun Oh, and In So Kweon. Image captioning with very scarce supervised data: Adversarial semi-supervised learning approach. In *Proceedings of the 2019 Conference on Empirical Methods in Natural Language Processing and the 9th International Joint Conference on Natural Language Processing (EMNLP-IJCNLP)*, 2019.
- [35] Dong-Jin Kim, Jinsoo Choi, Tae-Hyun Oh, Youngjin Yoon, and In So Kweon. Disjoint multi-task learning between heterogeneous human-centric tasks. In *IEEE Winter Conference on Applications of Computer Vision (WACV)*, 2018.
- [36] Dong-Jin Kim, Tae-Hyun Oh, Jinsoo Choi, and In So Kweon. Dense relational image captioning via multi-task triple-stream networks. *arXiv preprint arXiv:2010.03855*, 2020.
- [37] Dong-Jin Kim, Xiao Sun, Jinsoo Choi, Stephen Lin, and In So Kweon. Detecting human-object interactions with action co-occurrence priors. In *European Conference on Computer Vision (ECCV)*, 2020.
- [38] Jaehyung Kim, Youngbum Hur, Sejun Park, Eunho Yang, Sung Ju Hwang, and Jinwoo Shin. Distribution aligning refinery of pseudo-label for imbalanced semi-supervised learning. *Advances in Neural Information Processing Systems (NeurIPS)*, 2020.
- [39] Thomas N Kipf and Max Welling. Semi-supervised classification with graph convolutional networks. In *International Conference on Learning Representations (ICLR)*, 2017.
- [40] Ranjay Krishna, Yuke Zhu, Oliver Groth, Justin Johnson, Kenji Hata, Joshua Kravitz, Stephanie Chen, Yannis Kalantidis, Li-Jia Li, David A Shamma, et al. Visual genome: Connecting language and vision using crowdsourced dense image annotations. *International Journal of Computer Vision (IJCV)*, 123(1):32–73, 2017.
- [41] Lubor Ladicky, Chris Russell, Pushmeet Kohli, and Philip HS Torr. Graph cut based inference with co-occurrence statistics. In *European Conference on Computer Vision (ECCV)*, 2010.
- [42] L'ubor Ladický, Chris Russell, Pushmeet Kohli, and Philip HS Torr. Inference methods for crfs with co-occurrence statistics. *International Journal of Computer Vision (IJCV)*, 103(2):213–225, 2013.
- [43] Xi Li and Hichem Sahbi. Superpixel-based object class segmentation using conditional random fields. In *IEEE International Conference on Acoustics, Speech and Signal Processing (ICASSP)*, 2011.
- [44] Yikang Li, Wanli Ouyang, and Xiaogang Wang. VIP-CNN: A visual phrase reasoning convolutional neural network for visual relationship detection. In *IEEE Conference on Computer Vision and Pattern Recognition (CVPR)*, 2017.
- [45] Yikang Li, Wanli Ouyang, Bolei Zhou, Jianping Shi, Chao Zhang, and Xiaogang Wang. Factorizable net: An efficient subgraph-based framework for scene graph generation. In *European Conference on Computer Vision (ECCV)*, 2018.
- [46] Yikang Li, Wanli Ouyang, Bolei Zhou, Kun Wang, and Xiaogang Wang. Scene graph generation from objects, phrases and region captions. In *IEEE International Conference on Computer Vision (ICCV)*, 2017.
- [47] Yong-Lu Li, Xinpeng Liu, Han Lu, Shiyi Wang, Junqi Liu, Jiefeng Li, and Cewu Lu. Detailed 2d-3d joint representation for human-object interaction. In *IEEE Conference on Computer Vision and Pattern Recognition (CVPR)*, 2020.
- [48] Yong-Lu Li, Siyuan Zhou, Xijie Huang, Liang Xu, Ze Ma, Hao-Shu Fang, Yanfeng Wang, and Cewu Lu. Transferable interactiveness knowledge for human-object interaction detection. In *IEEE Conference on Computer Vision and Pattern Recognition (CVPR)*, 2019.
- [49] Zhizhong Li and Derek Hoiem. Learning without forgetting. In *European Conference on Computer Vision (ECCV)*, 2016.
- [50] Yue Liao, Si Liu, Fei Wang, Yanjie Chen, and Jiashi Feng. Ppdm: Parallel point detection and matching for real-time human-object interaction detection. In *IEEE Conference on Computer Vision and Pattern Recognition (CVPR)*, 2020.
- [51] Tsung-Yi Lin, Michael Maire, Serge Belongie, James Hays, Pietro Perona, Deva Ramanan, Piotr Dollár, and C Lawrence Zitnick. Microsoft coco: Common objects in context. In *European Conference on Computer Vision (ECCV)*, 2014.
- [52] Y Liu, Q Chen, and A Zisserman. Amplifying key cues for human-object-interaction detection. In *European Conference on Computer Vision (ECCV)*, 2020.

- [53] Cewu Lu, Ranjay Krishna, Michael Bernstein, and Li Fei-Fei. Visual relationship detection with language priors. In *European Conference on Computer Vision (ECCV)*, 2016.
- [54] Marcin Marszałek and Cordelia Schmid. Semantic hierarchies for visual object recognition. In *IEEE Conference on Computer Vision and Pattern Recognition (CVPR)*, 2007.
- [55] George A Miller. Wordnet: a lexical database for english. *Communications of the ACM*, 38(11):39–41, 1995.
- [56] Roozbeh Mottaghi, Xianjie Chen, Xiaobai Liu, Nam-Gyu Cho, Seong-Whan Lee, Sanja Fidler, Raquel Urtasun, and Alan Yuille. The role of context for object detection and semantic segmentation in the wild. In *IEEE Conference on Computer Vision and Pattern Recognition (CVPR)*, 2014.
- [57] Youngtaek Oh, Dong-Jin Kim, and In So Kweon. Distribution-aware semantics-oriented pseudo-label for imbalanced semi-supervised learning. *arXiv preprint arXiv:2106.05682*, 2021.
- [58] Jeffrey Pennington, Richard Socher, and Christopher Manning. Glove: Global vectors for word representation. In *Conference on Empirical Methods in Natural Language Processing (EMNLP)*, 2014.
- [59] Julia Peyre, Ivan Laptev, Cordelia Schmid, and Josef Sivic. Detecting unseen visual relations using analogies. In *IEEE International Conference on Computer Vision (ICCV)*, 2019.
- [60] Bryan A Plummer, Arun Mallya, Christopher M Cervantes, Julia Hockenmaier, and Svetlana Lazebnik. Phrase localization and visual relationship detection with comprehensive linguistic cues. *IEEE International Conference on Computer Vision (ICCV)*, 2017.
- [61] Mengshi Qi, Weijian Li, Zhengyuan Yang, Yunhong Wang, and Jiebo Luo. Attentive relational networks for mapping images to scene graphs. In *IEEE Conference on Computer Vision and Pattern Recognition (CVPR)*, 2019.
- [62] Siyuan Qi, Wenguan Wang, Baoxiong Jia, Jianbing Shen, and Song-Chun Zhu. Learning human-object interactions by graph parsing neural networks. In *European Conference on Computer Vision (ECCV)*, 2018.
- [63] Shaoqing Ren, Kaiming He, Ross Girshick, and Jian Sun. Faster R-CNN: Towards real-time object detection with region proposal networks. In *Advances in Neural Information Processing Systems (NeurIPS)*, 2015.
- [64] Liyue Shen, Serena Yeung, Judy Hoffman, Greg Mori, and Li Fei-Fei. Scaling human-object interaction recognition through zero-shot learning. In *IEEE Winter Conference on Applications of Computer Vision (WACV)*, 2018.
- [65] Louise Stark and Kevin Bowyer. Achieving generalized object recognition through reasoning about association of function to structure. *IEEE Transactions on Pattern Analysis and Machine Intelligence (TPAMI)*, 13(10):1097–1104, 1991.
- [66] Li Sulimowicz, Ishfaq Ahmad, and Alexander Aved. Superpixel-enhanced pairwise conditional random field for semantic segmentation. In *IEEE International Conference on Image Processing (ICIP)*, 2018.
- [67] Xiao Sun, Chuankang Li, and Stephen Lin. Explicit spatiotemporal joint relation learning for tracking human pose. In *Proceedings of the IEEE International Conference on Computer Vision Workshops*, 2019.
- [68] Xiao Sun, Yichen Wei, Shuang Liang, Xiaoou Tang, and Jian Sun. Cascaded hand pose regression. In *IEEE Conference on Computer Vision and Pattern Recognition (CVPR)*, 2015.
- [69] Charles Sutton and Andrew McCallum. An introduction to conditional random fields for relational learning. *Introduction to statistical relational learning*, 2:93–128, 2006.
- [70] Kaihua Tang, Yulei Niu, Jianqiang Huang, Jiabin Shi, and Hanwang Zhang. Unbiased scene graph generation from biased training. In *IEEE Conference on Computer Vision and Pattern Recognition (CVPR)*, 2020.
- [71] Oytun Ulutan, ASM Iftekhar, and BS Manjunath. Vsgnet: Spatial attention network for detecting human object interactions using graph convolutions. In *IEEE Conference on Computer Vision and Pattern Recognition (CVPR)*, 2020.
- [72] Phong D Vo and Hichem Sahbi. Modeling label dependencies in kernel learning for image annotation. In *IEEE International Conference on Image Processing (ICIP)*, 2014.
- [73] Bo Wan, Desen Zhou, Yongfei Liu, Rongjie Li, and Xuming He. Pose-aware multi-level feature network for human object interaction detection. In *IEEE International Conference on Computer Vision (ICCV)*, 2019.
- [74] Hai Wang, Wei-shi Zheng, and Ling Yingbiao. Contextual heterogeneous graph network for human-object interaction detection. In *European Conference on Computer Vision (ECCV)*, 2020.
- [75] Tiancai Wang, Rao Muhammad Anwer, Muhammad Haris Khan, Fahad Shahbaz Khan, Yanwei Pang, Ling Shao, and Jorma Laaksonen. Deep contextual attention for human-object interaction detection. In *IEEE International Conference on Computer Vision (ICCV)*, 2019.
- [76] Tiancai Wang, Tong Yang, Martin Danelljan, Fahad Shahbaz Khan, Xiangyu Zhang, and Jian Sun. Learning human-object interaction detection using interaction points. In *IEEE Conference on Computer Vision and Pattern Recognition (CVPR)*, 2020.
- [77] Wenbin Wang, Ruiping Wang, Shiguang Shan, and Xilin Chen. Exploring context and visual pattern of relationship for scene graph generation. In *IEEE Conference on Computer Vision and Pattern Recognition (CVPR)*, 2019.
- [78] Xiaolong Wang, Ross Girshick, Abhinav Gupta, and Kaiming He. Non-local neural networks. In *IEEE Conference on Computer Vision and Pattern Recognition (CVPR)*, 2018.
- [79] Sanghyun Woo, Dahun Kim, Donghyeon Cho, and In So Kweon. Linknet: Relational embedding for scene graph. In *Advances in Neural Information Processing Systems (NeurIPS)*, 2018.
- [80] Bingjie Xu, Junnan Li, Yongkang Wong, Qi Zhao, and Mohan S Kankanhalli. Interact as you intend: Intention-driven human-object interaction detection. *IEEE Transactions on Multimedia*, 2019.
- [81] Bingjie Xu, Yongkang Wong, Junnan Li, Qi Zhao, and Mohan S Kankanhalli. Learning to detect human-object interactions with knowledge. In *IEEE Conference on Computer Vision and Pattern Recognition (CVPR)*, 2019.
- [82] Danfei Xu, Yuke Zhu, Christopher B Choy, and Li Fei-Fei. Scene graph generation by iterative message passing. In *IEEE International Conference on Computer Vision (ICCV)*, 2017.
- [83] Zhicheng Yan, Hao Zhang, Robinson Piramuthu, Vignesh Jagadeesh, Dennis DeCoste, Wei Di, and Yizhou Yu. Hd-cnn: hierarchical deep convolutional neural networks for large scale visual recognition. In *IEEE International Conference on Computer Vision (ICCV)*, 2015.
- [84] Jianwei Yang, Jiasen Lu, Stefan Lee, Dhruv Batra, and Devi Parikh. Graph r-cnn for scene graph generation. In *European Conference on Computer Vision (ECCV)*, 2018.
- [85] Xu Yang, Hanwang Zhang, and Jianfei Cai. Shuffle-then-assemble: learning object-agnostic visual relationship features. In *European Conference on Computer Vision (ECCV)*, 2018.
- [86] Bangpeng Yao and Li Fei-Fei. Grouplet: A structured image representation for recognizing human and object interactions. In *IEEE Conference on Computer Vision and Pattern Recognition (CVPR)*, 2010.
- [87] Bangpeng Yao and Li Fei-Fei. Modeling mutual context of object and human pose in human-object interaction activities. In *IEEE Conference on Computer Vision and Pattern Recognition (CVPR)*, 2010.
- [88] Bangpeng Yao, Xiaoye Jiang, Aditya Khosla, Andy Lai Lin, Leonidas Guibas, and Li Fei-Fei. Human action recognition by learning bases of action attributes and parts. In *IEEE International Conference on Computer Vision (ICCV)*, 2011.
- [89] Jian Yao, Sanja Fidler, and Raquel Urtasun. Describing the scene as a whole: Joint object detection, scene classification and semantic segmentation. In *IEEE Conference on Computer Vision and Pattern Recognition (CVPR)*, 2012.
- [90] Ting Yao, Yingwei Pan, Yehao Li, and Tao Mei. Exploring visual relationship for image captioning. In *European Conference on Computer Vision (ECCV)*, 2018.
- [91] Guojun Yin, Lu Sheng, Bin Liu, Nenghai Yu, Xiaogang Wang, Jing Shao, and Chen Change Loy. Zoom-net: Mining deep feature interactions for visual relationship recognition. In *European Conference on Computer Vision (ECCV)*, 2018.
- [92] Ruichi Yu, Ang Li, Vlad I Morariu, and Larry S Davis. Visual relationship detection with internal and external linguistic knowledge distillation. In *IEEE International Conference on Computer Vision (ICCV)*, 2017.
- [93] Rowan Zellers, Mark Yatskar, Sam Thomson, and Yejin Choi. Neural motifs: Scene graph parsing with global context. In *IEEE Conference on Computer Vision and Pattern Recognition (CVPR)*, 2018.
- [94] Yibing Zhan, Jun Yu, Ting Yu, and Dacheng Tao. On exploring undetermined relationships for visual relationship detection. In *IEEE Conference on Computer Vision and Pattern Recognition (CVPR)*, 2019.
- [95] Hanwang Zhang, Zawlin Kyaw, Shih-Fu Chang, and Tat-Seng Chua. Visual translation embedding network for visual relation detection. In *IEEE Conference on Computer Vision and Pattern Recognition (CVPR)*, 2017.
- [96] Hang Zhang, Han Zhang, Chenguang Wang, and Junyuan Xie. Co-occurrent features in semantic segmentation. In *IEEE Conference on Computer Vision and Pattern Recognition (CVPR)*, 2019.
- [97] Ji Zhang, Mohamed Elhoseiny, Scott Cohen, Walter Chang, and Ahmed Elgammal. Relationship proposal networks. In *IEEE Conference on Computer Vision and Pattern Recognition (CVPR)*, 2017.
- [98] Xubin Zhong, Changxing Ding, Xian Qu, and Dacheng Tao. Polysemy deciphering network for human-object interaction detection. In *European Conference on Computer Vision (ECCV)*, 2020.

- [99] Penghao Zhou and Mingmin Chi. Relation parsing neural network for human-object interaction detection. In *IEEE International Conference on Computer Vision (ICCV)*, 2019.
- [100] Bohan Zhuang, Lingqiao Liu, Chunhua Shen, and Ian Reid. Towards context-aware interaction recognition for visual relationship detection. In *IEEE Conference on Computer Vision and Pattern Recognition (CVPR)*, 2017.
- [101] Bohan Zhuang, Qi Wu, Chunhua Shen, Ian Reid, and Anton van den Hengel. Hcvrd: a benchmark for large-scale human-centered visual relationship detection. In *AAAI Conference on Artificial Intelligence (AAAI)*, 2018.



**Dong-Jin Kim** received the B.S. degree, M.S. degree, and Ph.D. degree in Electrical Engineering from Korea Advanced Institute of Science and Technology (KAIST), Daejeon, South Korea, in 2015, 2017, and 2021, respectively. He was a research intern in the Visual Computing Group, Microsoft Research Asia (MSRA). He was awarded a silver prize from Samsung Humantech paper awards and Qualcomm Innovation awards. His research interests include high-level computer vision such as language and vision and human behavior understanding. He

is a student member of the IEEE.



**In So Kweon** received the BS and MS degrees in mechanical design and production engineering from Seoul National University, Seoul, South Korea, in 1981 and 1983, respectively, and the PhD degree in robotics from the Robotics Institute, Carnegie Mellon University, Pittsburgh, Pennsylvania, in 1990. He is an professor with the Electrical Engineering Department, KAIST, South Korea. He worked for the Toshiba R&D Center, Japan, and joined the Department of Automation and Design Engineering, KAIST, Seoul, South Korea, in 1992, where he is currently a professor with the Department of Electrical Engineering. He is a recipient of the Best Student Paper Runner-up Award at the IEEE Conference on Computer Vision and Pattern Recognition (CVPR 09). His research interests include camera and 3D sensor fusion, color modeling and analysis, visual tracking, and visual SLAM. He was the program co-chair for the Asian Conference on Computer Vision (ACCV 07) and was the general chair for the ACCV 12. He is also on the editorial board of the International Journal of Computer Vision. He is a member of the IEEE and KROS.

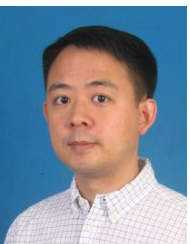


**Xiao Sun** is a Senior Researcher in the Visual Computing Group of Microsoft Research Asia. He received the B.S. and M.S. degrees in Information Engineering from South China University of Technology, China, in 2011 and 2014, respectively. His research interests include computer vision and machine learning, especially pose estimation, object detection and action recognition.



**Jinsoo Choi** received his B.S., M.S., and Ph.D. degrees in Electrical Engineering from Korea Advanced Institute of Science and Technology (KAIST) in 2013, 2015, and 2020 respectively. He received the grand prize from the Electronic Times paper awards hosted by the Ministry of Science and ICT, Rep. of Korea, silver prize from Samsung Electro-Mechanics paper awards, silver prize from Samsung Humantech paper awards, Qualcomm Innovation awards, recognition as top research achievements and top 1% research achievements from KAIST

annual and biannual R&D reports. His research interests include deep learning, computer vision, and computer graphics with an emphasis on video enhancement and processing.



**Stephen Lin** is a Senior Principal Research Manager in the Visual Computing Group of Microsoft Research Asia. He obtained a B.S.E. from Princeton University and a Ph.D. from the University of Michigan. His research interests include computer vision and computer graphics. Dr. Lin is on the editorial board of the International Journal of Computer Vision, and has served as a program chair for the International Conference on 3D Vision 2020, International Conference on Computer Vision 2011, and Pacific-Rim Symposium on Image and Video

Technology 2009.